Atomic structure, mechanical quality, and thermodynamic property of TiHx phases

Article *in* Journal of Applied Physics · July 2013

DOI: 10.1063/1.4816485

2 authors:

C. P. Liang
Central South University
82 PUBLICATIONS **1,207** CITATIONS
SEE PROFILE

Haoran Gong
Central South University
89 PUBLICATIONS **999** CITATIONS
SEE PROFILE

Atomic structure, mechanical quality, and thermodynamic property of TiHx phases

C. P. Liang and H. R. Gong

Citation: J. Appl. Phys. **114**, 043510 (2013); doi: 10.1063/1.4816485
View online: http://dx.doi.org/10.1063/1.4816485
View Table of Contents: http://jap.aip.org/resource/1/JAPIAU/v114/i4
Published by the AIP Publishing LLC.

JOURNAL OF APPLIED PHYSICS **114**, 043510 (2013)

Atomic structure, mechanical quality, and thermodynamic property of TiH_x phases

C. P. Liang and H. R. Gong[a)]
State Key Laboratory of Powder Metallurgy, Central South University, Changsha, Hunan 410083, China

(Received 15 May 2013; accepted 8 July 2013; published online 25 July 2013)

Titanium hydrides TiH_x ($x = 1$, 1.25, 1.5, 1.75, and 2) with the cubic fluorite-type (face-centered cubic, δ phase) and face-centered-tetragonal (ε phase, $c/a < 1$; γ phase, $c/a > 1$) structures were systematically investigated and compared through first-principles calculation. The H location of TiH_x was carefully determined by comparing the calculated properties with experimental results. Moreover, the mechanical properties of ε and γ phases were calculated and found to play an important role in the brittle/ductile behavior of TiH_x phases. In addition, the thermodynamic quantities were also derived for providing a deeper understanding of TiH_x phases. The calculated results were widely compared with the available experimental results in the literature, and could clarify the three controversies regarding atomic configuration, stability, and hydrogen embrittlement of TiH_x phases in the literature. © *2013 AIP Publishing LLC*.
[http://dx.doi.org/10.1063/1.4816485]

I. INTRODUCTION

During the past years, the metal titanium (Ti) and its hydrides have been used as promising materials in hydrogen storage and various structural applications.[1–4] It is well believed that the titanium hydrides TiH_x ($1 \le x \le 2$) possess mainly three structures, i.e., face-centered cubic phase (FCC, δ phase), and two face-centered-tetragonal structures (FCT, c/a $>$ 1, γ phase; c/a $<$ 1, ε phase).[2–17] Interestingly, phase transitions between these δ, γ, and ε structures could be triggered as a function of temperature or hydrogen composition, and our recent study revealed the fundamental mechanism of tetragonal transitions in titanium hydrides.[18]

The H configuration in TiH_x phases, however, has been controversial for many years in the literature.[5,10–12,16] For instance, some experiments showed that H atoms are randomly occupying the interstitial positions of TiH_x phases,[5] while an ordered arrangement of H is found by other experimentalists.[16] On the other hand, the atomic configurations of H in $TiH_{1.5}$ from various theoretical calculations are quite different from each other.[10–12] Fundamentally, there should exist an intrinsic configuration of H atoms in each TiH_x phase, and such an atomic configuration should be irrelevant to experimental and theoretical methods.

As to the stability of γ TiH phases, the experimental and calculational results in the literature are also not consistent with each other.[12–23] Specifically, γ phases could not be found in several phase diagrams of Ti-H,[13–15] while do exist in other Ti-H phase diagrams.[2–4] In addition, first principles calculation by Xu and Van der Ven showed that γ TiH phases are unstable,[12] whereas San-Martin and Manchester believed that γ TiH structures are metastable.[13] On the contrary, a lot of experimental studies confirmed the existence of stable γ TiH phases.[2,16,17,19–22]

Another controversy of TiH_x phases in the literature is about hydrogen embrittlement.[24–30] For instance, many authors believed that δ or γ TiH_x phases are responsible for hydrogen embrittlement,[24,26–28] while others found that the γ structure has a considerable plastic accommodation,[24] and the δ phase can be deformed plastically to enhance the local ductility.[29,30] However, there is a lack of a systematic study of mechanical properties of δ, γ, and ε TiH_x phases, and the intrinsic effects of H are still unknown to the research society.

By means of first principles calculations, the present study is, therefore, aimed to clarify the above controversies in the literature, and to systematically investigate the atomic structure, mechanical quality, and thermodynamic properties of δ, γ, and ε TiH_x phases within a wide composition range ($1 \le x \le 2$).

II. THEORETICAL METHODS

The first-principles calculation is based on the well-established Vienna *ab initio* simulation package (VASP) within the density functional theory.[31] The calculation is conducted in a plane-wave basis, using the projector-augmented wave (PAW) method.[32] The exchange and correlation items are described by generalized gradient approximation (GGA) of Perdew *et al.*,[33] and the cutoff energies are 450 and 600 eV for plane wave basis and augmentation charge, respectively. For k space integration, the temperature smearing method of Methfessel-Paxton[34] was used for dynamical calculation and the modified tetrahedron method of Blöchl-Jepsen-Andersen[35] was performed for static calculation.

Accordingly, a unit cell of 4 Ti atoms with the FCC structure was used as the starting structure for the TiH_x phase and a series of H atoms were added at the tetrahedral interstitial sites of the FCC unit, i.e., the addition of 4, 5, 6, 7, and 8 H atoms stands for the TiH, $TiH_{1.25}$, $TiH_{1.5}$, $TiH_{1.75}$, and

a)Author to whom correspondence should be addressed. Electronic mail: gonghr@csu.edu.cn. Tel.: +86 731 88877387. Fax: +86 731 88710855.

TiH_2 phases, respectively. At each composition, all possible configurations of H atoms were calculated in terms of atomic volume, in order to find out the optimized lattice constants as well as the structural energy differences. For the crystal structure, Fig. 1 shows the schematic picture of the FCC unit cell of TiH_x ($1 \leq x \leq 2$), and the H atoms at the tetrahedral sites are purposely lettered to provide a clear description of various atomic configurations. To obtain the ground-state FCT TiH_x phases, the original c/a value of 1 for each FCC structure (δ phase) is varied from 0.80 to 1.20 with an interval of 0.01. At each c/a ratio, the volume and inter-atomic positions are allowed for full relaxation, while the crystal shape keeps constant during calculation.

Lattice dynamics calculations are carried out in the framework of the supercell approach using a small displacement method as implemented in the PHONOPY code.[36] A supercell model of $2 \times 2 \times 2$ is chosen for each δ TiH_x phase. After a series of test calculations, the k-meshes of $15 \times 15 \times 15$, $21 \times 21 \times 21$, and $7 \times 7 \times 7$ are selected for dynamic, elastic constants, and supercell calculations, respectively. The energy criteria are 0.01 and 0.1 meV for electronic and ionic relaxations, respectively, while 0.001 meV for the calculation of density of states (DOS) and elastic constants.

III. RESULTS AND DISCUSSION

A. Atomic structure

After the calculation, the structural energy differences of δ TiH_x phases with various atomic configurations of H are derived and listed in Table I. It should be pointed out that the combination of letters (a–h) in Fig. 1 is used to express the atomic configuration of H, e.g., the symbol of (*abcd*) for the δ TiH phase means that the 4 H atoms are at the tetrahedral interstitial sites of a, b, c, and d shown in Fig. 1. One sees clearly from Table I that there is only one H configuration for each $TiH_{1.75}$ and TiH_2 phase, and that the energetically preferable configurations of H for TiH, $TiH_{1.25}$, and $TiH_{1.5}$ are (*abgh*), (*abceg*), and (C_3:*abcdef*), respectively. In addition, calculation also reveals that the energetically preferable configuration of H for each FCT (γ or ε) TiH_x phase is just the same as that shown in Table I for δ TiH_x phases, which seems consistent with corresponding experimental and theoretical observations in the literature.[10–12,16–19] Interestingly, the structural energy differences (ΔE) between various H atomic configurations shown in Table I become smaller with the increase of the H concentration, i.e., 0.42 eV for TiH, 0.15 eV for $TiH_{1.25}$, while 0.02 eV for $TiH_{1.5}$. Such a smaller structural energy difference implies that the diffusion of H atoms between different configurations of δ TiH_x phases would probably become easier with the increase of H concentration.

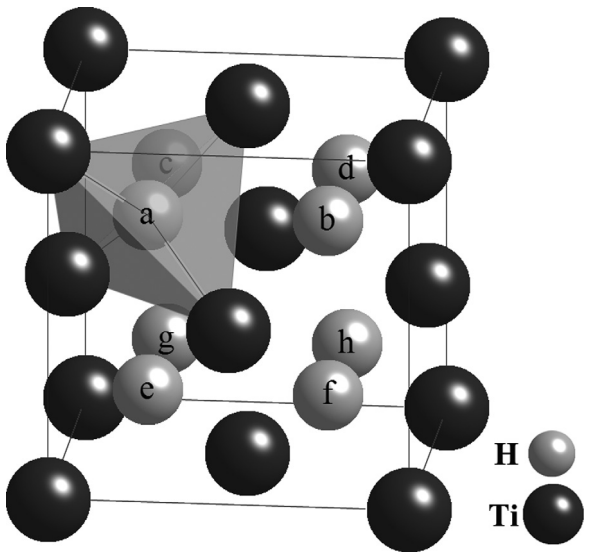

FIG. 1. Schematic picture of the FCC unit cell of the titanium hydrides TiH_x ($1 \leq x \leq 2$) phase. The small spheres lettered a–h stand for H atoms located at the tetrahedral interstitials of the FCC lattice.

The lattice constants of FCC TiH_x phases with various atomic configurations of H are summarized in Table I, and the lattice parameters (a, c, and c/a) of energetically favorable FCT phases are listed in Table II. In addition, the available lattice constants of FCC and FCT TiH_x phases from experiments in the literature[16–19,37–45,56] are also included in Tables I and II for the sake of comparison. It could be seen from Tables I and II that the present results are in good agreement with the experimental data. For instance, the lattice constants of δ $TiH_{1.5}$ (4.391, 4.395, and 4.397 Å) from the present calculation match well with the corresponding experimental values of 4.40 Å (Ref. 39) and 4.405 Å.[40] In addition, the present lattice constants ($a = 4.164$ Å, $c = 4.581$ Å) of γ TiH are consistent with corresponding data from experiments, i.e., $a = 4.199$ Å, $c = 4.576$ Å;[37] $a = 4.21$ Å, $c = 4.6$ Å;[16] $a = 4.19$ Å, $c = 4.69$ Å.[38]

We now investigate the ground-state atomic configuration of the δ $TiH_{1.5}$ phase. It can be seen from Table I that there are three atomic configurations of H for $TiH_{1.5}$, i.e., C_1: *abcfgh*, C_2: *abcdeg*, and C_3: *abcdef*, and that the structural energy differences (ΔE) between these three configurations are very small values of less than 0.02 eV per unit cell. Such a small energy difference suggests that it seems difficult to differentiate which is the ground-state configuration from the energetic point of view. As mentioned before, there is a controversy regarding the ground-state atomic configuration of TiH_x phases in the literature,[5,10–12,16] e.g., for the δ $TiH_{1.5}$ phase, the calculated ground-state atomic configuration from Tao *et al.*[10] and Xu *et al.*[12] is C_1, while C_3 from Wang *et al.*[11]

It is of importance to clarify the above controversy regarding ground state of δ $TiH_{1.5}$ from electronic structures. As typical examples, Fig. 2 shows the comparison of total DOS of the FCC (δ) $TiH_{1.5}$ phases with H configurations of C_1 and C_3, as well as the corresponding curve from experiments.[46] It can be observed from Fig. 2 that the Fermi level (E_f) of C_1 is located near the DOS peak and the energy state at E_f is a high value of 7.92 (states/eV/unit cell). On the contrary, the E_f of C_2 (figure not shown) and C_3 are situated at the bottom of the pseudo-gap of DOS peaks, and the energy states at E_f are much smaller values of 4.12 and 3.01 (states/eV/unit cell) for C_2 and C_3, respectively. It should be noted that the experimental results of δ $TiH_{1.5}$ in the literature[7–9,40,46] show a minimum of energy states at E_f, which agrees well with C_2 and C_3, while contradictory to C_1,

TABLE I. Lattice constant a, structural energy difference ΔE, and heat of formation ΔH_f of δ TiH_x phases with various atomic configurations of H. The boldface values denote the calculated ground-state structure of δ TiH_x. The experimental and calculational results in the literature are also included for comparison.[37,39–41,46,47,54] Please see the details of the unit cell and H positions in Fig. 1 and the text.

		a (Å)			ΔH_f (kJ/mol)	
Phases	Atomic configurations of H	This study	Exp.	ΔE (eV/unit cell)	This study	Cal.
TiH	*a b c d*	4.352	4.4 (Ref. 39)	0.42	−68.29	−71.58;[55]
	a b g h	**4.326**		**0.00**	**−78.31**	−80 (Ref. 54)
	a c d e	4.337		0.15	−74.59	
	a c d g	4.350		0.42	−68.10	
	a c d f	4.335		0.12	−75.34	
$TiH_{1.25}$	*a b c d g*	4.375	4.4 (Ref. 39)	0.15	−94.20	
	a b c f h	4.372		0.15	−94.32	
	a b c e g	**4.363**		**0.00**	**−97.90**	
$TiH_{1.5}$	**C_1**: *a b c f g h*	4.391	4.4 (Ref. 39)	0.02	−118.41	−107.19 (Ref. 55)
	C_2: *a b c d e g*	4.395	4.405 (Ref. 40)	0.01	−118.57	
	C_3: *a b c d e f*	**4.397**		**0.00**	**−118.80**	
$TiH_{1.75}$	*a b c d e g h*	4.416	4.423 (Ref. 39)	0.00	−140.09	−124.85 (Ref. 55)
			4.427 (Ref. 40)			
TiH_2	*a b c d e f g h*	4.437	4.44 (Ref. 37)	0.00	−160.15	−142.39 (Ref. 55)
			4.454 (Ref. 41)			−165 (Ref. 51)

suggesting that C_1 should not be the ground state of δ $TiH_{1.5}$. In addition, the peaks and shoulders of DOS curves from experiments in the literature[46] are located at about −7.3, −5.1, −1.5, −0.9, and −0.2 eV below E_f, which are very similar to the features of DOSs of C_3 shown in Fig. 2, while different from those DOSs of C_1 and C_2, indicating that C_1 and C_2 should not be the ground state of δ $TiH_{1.5}$. All the above features of E_f and DOS peaks imply that C_3 should be the ground-state atomic configuration of δ $TiH_{1.5}$, and such a statement could give a reasonable explanation to the above-mentioned controversy regarding ground state of δ TiH_x phases in the literature.[5,10–12,16] It should be pointed out that the atomic structure of δ TiH_x at higher temperature would be probably complicated and further study is needed, as H atoms would diffuse more easily between different atomic configurations due to very small structural energy difference and high diffusivity.

TABLE II. Lattice parameters (a, c, and c/a) and heat of formation (ΔH_f) of energetically favorable FCT TiH_x phases. The available experimental data are also listed for comparison.[16,37,38,40–45] The H configurations in TiH and $TiH_{1.25}$ are (*abgh*) and (*abceg*), respectively.

			Lattice parameters			
Phases	Method	Structure	a (Å)	c(Å)	c/a	ΔH_f (kJ/mol)
TiH	This study	γ	4.164	4.581	1.10	−81.78
	Exp.[16]	γ	4.21	4.6	1.09	
	Exp.[37]	γ	4.199	4.576	1.09	
	Exp.[38]	γ	4.19	4.69	1.12	
$TiH_{1.25}$	This study	γ	4.226	4.564	1.08	−99.37
$TiH_{1.5}$	This study	**C_1**: ε	4.487	4.128	0.92	−118.62
		C_2: γ	4.343	4.430	1.02	−118.66
		C_3: γ	4.360	4.404	1.01	−118.83
$TiH_{1.75}$	This study	ε	4.467	4.244	0.95	−140.19
	Exp.[42]	ε	4.470	4.397	0.98	
	Exp.[43]	ε	4.475	4.372	0.98	
TiH_2	This study	ε	4.517	4.201	0.93	−160.32
	Exp.[41]	ε	4.528	4.279	0.95	
	Exp.[43]	ε	4.499	4.37	0.97	
	Exp.[44]	ε	4.49	4.36	0.97	
	Exp.[45]	ε	4.483	4.365	0.97	
	Exp.[40]	ε	4.485	4.36	0.97	

To probe the thermodynamic stability of TiH_x phases, the heat of formation, ΔH_f, is calculated according to the following formula:

$$\Delta H_f = E_{TiH_x} - E_{Ti} - \frac{x}{2}E_{H_2}, \quad (1)$$

where E_{TiHx}, E_{Ti}, and E_{H_2} are total energies of TiH_x, pure α-Ti (ground state), and H_2 molecules, respectively.

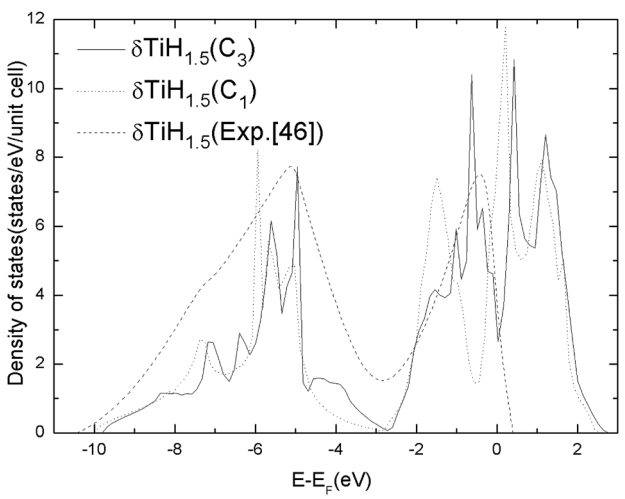

FIG. 2. Comparison of total density of states of the FCC (δ) $TiH_{1.5}$ phases with H configurations of C_1 and C_3. The corresponding curve from experiments[46] is also included.

Accordingly, the derived ΔH_f values of FCC TiH_x phases with various atomic configurations of H are listed in Table I, and the ΔH_f of FCT and FCC TiH_x phases with energetically favorable H configurations are shown in Table II and Fig. 3, respectively. In addition, the corresponding experimental[15,47–53] and calculated[54,55] results in the literature are also included for the sake of comparison.

Several characteristics could be detected from Tables I and II as well as Fig. 3. First, it can be seen that the calculated ΔH_f of δ TiH_x phases from the present study are consistent with experimental and calculated results available in the literature.[15,47–55] For instance, the present ΔH_f value of δ TiH_2 is −160.15 kJ/(mol Ti), which agrees well with the calculated value of −165 kJ/(mol Ti).[51] Second, it can be seen from Table I that the ΔH_f of all investigated FCC and FCT TiH_x phases are big and negative values within the range of −68 to −160 kJ/(mol Ti), suggesting that all these phases should be energetically favorable.

Third, it could be observed from Fig. 3 that the ΔH_f values decrease almost linearly with the increase of H concentration, and such a linear change of ΔH_f with H concentration matches well with experimental and theoretical evidence in the literature.[47–55] Fourth, for both FCC and FCT structures, the differences of ΔH_f between three H atomic configurations of $TiH_{1.5}$ seem very small, implying that atomic structures of H should have negligible effect on energetics of $TiH_{1.5}$ phases. It should be mentioned that such an observation of $TiH_{1.5}$ would be quite different from the cases of TiH and $TiH_{1.25}$ shown in Table I.

As related before, there exists a controversy regarding the stability of γ TiH phases in the literature, i.e., unstable,[12] metastable,[13] and stable.[16,17,19–22] For each TiH, $TiH_{1.25}$, and $TiH_{1.5}$ phase, it could be discerned from Tables I and II that the γ structure has a little bit lower ΔH_f value than the corresponding δ structure. Moreover, the γ TiH_x phases are energetically favorable with big and negative ΔH_f values of −81 to −118 kJ/(mol Ti) as shown in Table II, and it will be revealed in Sec. III B that these γ TiH_x phases are all mechanically stable. Considering all the above points together, a conclusion would be probably drawn that the γ TiH, $TiH_{1.25}$, and $TiH_{1.5}$ phases should be stable, instead of metastable or unstable. Such a stable feature of γ TiH_x phase is not only in good agreement with experimental observations,[16,17,19–22] but also could clarify the above-mentioned controversy in the literature.[12–23] In addition, the ΔH_f of the δ and γ $TiH_{1.5}$ phases with the H configuration of C_3 are very close values of −118.80 and −118.83 kJ/(mol Ti) as shown in Tables I and II, suggesting that the δ and γ structures of $TiH_{1.5}$ would probably co-existed, which matches well with similar observation of the coexistence of δ and γ $TiH_{1.5}$ from experiments.[17]

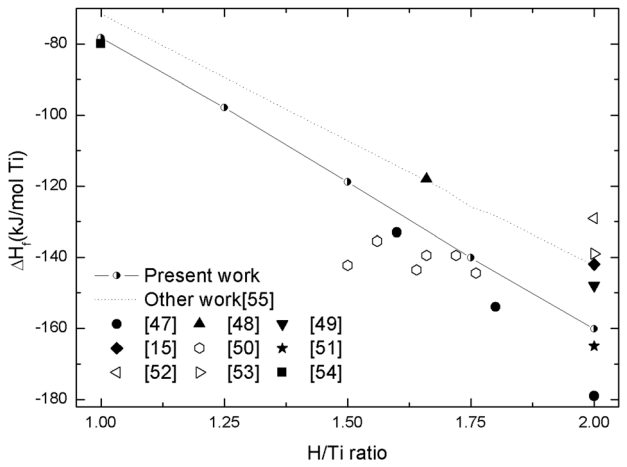

FIG. 3. Heats of formation of δ TiH_x ($1 \le x \le 2$) phases with energetically favorable H configurations. The experimental[47–53] and calculated[54,55] results in the literature are also listed for comparison.

B. Mechanical quality

We turn to reveal mechanical stabilities of TiH_x($1 \le x \le 2$) phases. According to the strain energy theory, for a mechanically stable phase the strain energy should be positive, and the matrix of elastic constants should be positive, definite, and symmetric,[57] which could be expressed for the cubic structure as: $C_{11} > 0$, $C_{11}^2 > C_{12}^2$, and $C_{44} > 0$, and for FCT structure: $C_{11} > 0$, $C_{11}^2 > C_{12}^2$, $C_{33}(C_{11} + C_{12}) > 2C_{13}^2$, $C_{11} \cdot C_{33} > C_{13}^2$, and C_{44}, $C_{66} > 0$. Specifically, the elastic constants are calculated according to the method proposed by Yu *et al.*,[58] and the main idea is presented as follows: we apply universal-linear-independent coupling-strains to the equilibrium lattice, determine the resulting change in stress, and from this information, deduce elastic constants of single crystals through the Hooke's law. After a series of calculation, Table III shows single crystal elastic constants (C_{11}, C_{12}, C_{13}, C_{33}, C_{44}, and C_{66}) of FCC and FCT TiH_x phases with energetically favorable H configurations. It could be detected from this table that the TiH and $TiH_{1.25}$ phases as well as the ε structures of $TiH_{1.75}$ and TiH_2 are all mechanically stable according to the strain energy theory, while the δ phases of $TiH_{1.75}$ and TiH_2 become mechanically unstable at 0 K with negative values of (C_{11}-C_{12}) or C_{44}.

For the $TiH_{1.5}$ phases, it could be seen from Table III that the atomic configuration of H has an importance on mechanical stability, i.e., the δ $TiH_{1.5}$ (C_1) phase possesses mechanical unstableness with a negative value of (C_{11}-C_{12}), and the γ $TiH_{1.5}$ (C_2) phase is also mechanically unstable as it disobeys the point of ($C_{11} \cdot C_{33} > C_{13}^2$), while the other structures including δ and γ $TiH_{1.5}$ (C_3) phases all have mechanical stability. The above characteristics regarding mechanical stability of $TiH_{1.5}$ shown in Table III further confirm the statement that C_3 should be the ground-state atomic configuration of the $TiH_{1.5}$ phases as revealed in Sec. III A.

It is of importance to probe the effects of H on elastic moduli of polycrystalline δ-TiH_x phases. The bulk (B), shear (G), and Young's (E) moduli are calculated using the Voigt's approximation[57]

$$B = \frac{1}{9}(C_{11} + C_{22} + C_{33}) + \frac{2}{9}(C_{12} + C_{13} + C_{23}), \quad (2)$$

$$G = \frac{1}{15}(C_{11} + C_{22} + C_{33}) - \frac{1}{15}(C_{12} + C_{13} + C_{23}) + \frac{1}{5}(C_{44} + C_{55} + C_{66}), \quad (3)$$

TABLE III. Single crystal elastic constants (C_{11}, C_{12}, C_{13}, C_{33}, C_{44}, and C_{66}) and polycrystalline moduli (B, G, and E) of FCC and FCT TiH_x phases with energetically favorable H configurations. All values are in the unit of GPa.

Phases	Structure	C_{11}	C_{33}	C_{12}	C_{13}	C_{44}	C_{66}	C_{11}-C_{12}	B	G	E
TiH_1	δ	138		112		103		26	121	67	169
	γ	139	218	133	93	101	103	6	126	73	183
$TiH_{1.25}$	δ	135		119		95		16	124	60	155
	γ	132	194	129	107	98	101	3	127	67	171
$TiH_{1.5}$	C_1: δ	112		141		66		−29	131	34	94
	C_2: δ	148		115		93		33	126	63	161
	C_3: δ	154		114		90		40	127	62	160
	C_1: ε	148	143	120	125	89	63	28	132	51	135
	C_2: γ	148	123	116	173	97	101	32	131	67	171
	C_3: γ	171	180	110	106	101	104	61	130	74	187
$TiH_{1.75}$	δ	125		141		48		−16	136	25	72
	ε	149	134	137	127	62	65	12	135	41	111
TiH_2	δ	97		159		−11		−62	138	−19	−60
	ε	165	157	150	116	51	87	15	139	45	121

$$E = 9BG/(3B + G). \quad (4)$$

The Poisson's ratio (v) is determined by B and G as follows:

$$v = \frac{(3B - 2G)}{2(3B + G)}. \quad (5)$$

After the calculation, Fig. 4 summarizes the calculated B, E, and G values of δ TiH_x phases with energetically favorable H configurations as well as available results in the literature.[56,59–61] It could be seen from Fig. 4 that the derived mechanical properties of δ TiH_x phases from the present study are in good agreement with corresponding experimental values.[56,59–61] For instance, the bulk moduli (B) of δ $TiH_{1.75}$ and TiH_2 phases are calculated to be 136 and 138 GPa, respectively, which match well with the corresponding data of 135 (Ref. 56) and 139 (Ref. 60) GPa from experiments. Moreover, the crossover between B and E is predicted to be H/Ti = 1.59 from present study, which is consistent with the value of H/Ti = 1.54 from experimental measurements.[56] It could be also deduced from Fig. 4 that H concentration has different effects on elastic moduli of δ TiH_x phases, i.e., with the increase of H concentration, B has a very small increase, while G and E have a little bit fluctuation when $1 \leq x \leq 1.5$, and decrease sharply as $1.5 \leq x \leq 2$.

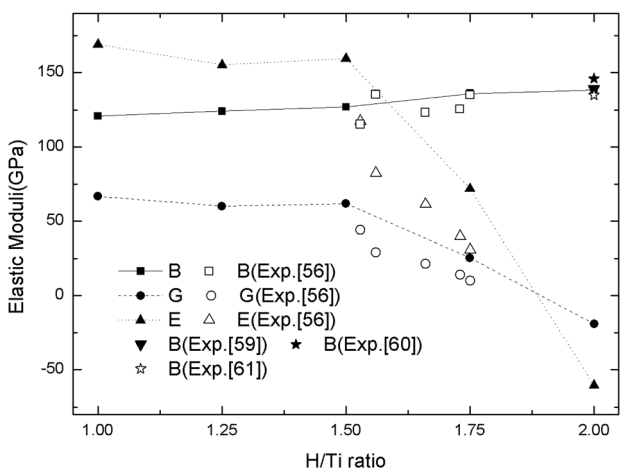

FIG. 4. Polycrystalline elastic moduli B, G, and E of δ TiH_x ($1 \leq x \leq 2$) phases with energetically favorable H configurations. The available experimental and calculated results in the literature[56,59–61] are also listed for comparison.

In addition, Table III lists the comparison of polycrystalline moduli (B, G, and E) of FCC and FCT TiH_x phases with energetically favorable H configurations. It could be observed from Table III that the polycrystalline elastic moduli (B, G, and E) of FCT TiH_x phases follow similar trends to those of δ-TiH_x with the increase of H concentration as related before. Generally speaking, for each TiH_x phase, it is of interest to see that the elastic modulus value (B, G, or E) of the FCT structure is bigger than that of the FCC structure, and such a feature of elastic moduli seems compatible with the smaller ΔH_f value of the FCT structure shown in Tables I and II.

To investigate the effect of H on brittle/ductile behavior of TiH_x phases, the G/B values of FCC and FCT TiH_x phases with energetically favorable H atomic configurations are calculated and shown in Fig. 5. It should be noted that the G/B value proposed by Pugh has been extensively used as an empirical parameter to express the brittleness/ductility of materials,[62] i.e., a bigger G/B value means more brittleness, and vice versa. First of all, it can be observed from Fig. 5 that for both FCC and FCT TiH_x phases there is a sharp decrease of the G/B values at the x of 1.5, and the fundamental reason of such a big change will be revealed later. Moreover, it could be also discerned from Fig. 5 that for each TiH_x phase, the FCT structure has a bigger G/B value than corresponding FCC structure, suggesting that the FCT TiH_x phase should be more brittle than its FCC counterpart.

In addition, one could deduce from Fig. 5 that H concentration has an important effect on the brittle/ductile behavior of both FCC and FCT TiH_x phases, i.e., brittle with big G/B values when $1 \leq x \leq 1.5$, while ductile with much smaller G/B as $1.5 < x \leq 2$. In other words, it is H concentration which induces the brittleness/ductility of FCC and FCT TiH_x

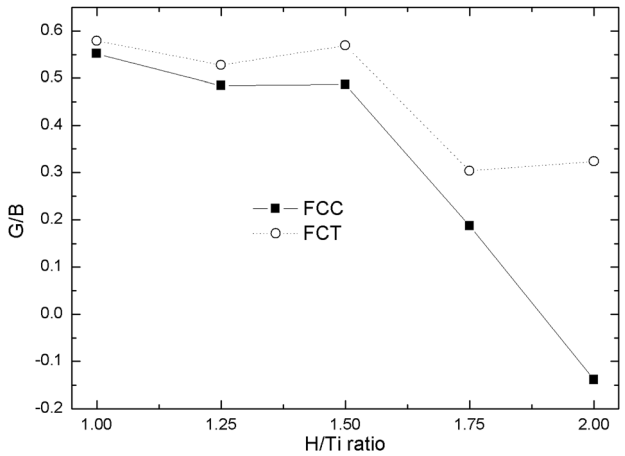

FIG. 5. The G/B ratios of FCC and FCT TiH_x phases with energetically favorable H atomic configurations.

phases, and such a statement revealed from the present study could therefore bring about a reasonable explanation to the previously related controversy regarding hydrogen embrittlement of δ or γ TiH_x phases in the literature,[24–30,63] i.e., δ or γ TiH_x phases with low hydrogen concentrations ($1 \leq x \leq 1.5$) would probably cause hydrogen embrittlement,[24,26–28] while δ or γ TiH_x phases with high hydrogen concentrations ($1.5 < x \leq 2$) would possibly become ductile to enhance plastic accommodation.[24,29,30]

It is of importance to find out the intrinsic mechanism of the effect of H on brittle/ductile behavior of TiH_x phases. Fig. 6 shows the electronic structures of various TiH_x phases as a function of H concentration. It could be observed from Fig. 6(a) that for the δ $TiH_{1.75}$ and TiH_2 phases, the Fermi level increases sharply to reach the DOS peak and the s electron of H atom (the peaks around -5.5 eV in the DOSs) becomes delocalized, which imply that the Ti-H bonding is mainly metallic. For the δ TiH_x phases ($x \leq 1.5$), however, the Fermi level is situated at or near the bottom of the pseudo-gap and the s electron of H atom has a strong localized profile around -5.5 eV and it is separated with Ti-d electrons by a gap at -3 eV, suggesting that the Ti-H bonding is mainly covalent. These DOS features of δ TiH_x phases indicate that a bonding transition from mainly covalent to mainly metallic should happen at $x = 1.5$. In other words, hydrogen concentration plays an important role in determining bonding features of δ TiH_x phases, which would then give a reasonable explanation to sharp decrease of the G/B values shown in Fig. 5 as related before.

Additionally, as shown in Fig. 6(b), the main features of DOSs for FCT TiH_x phases at $x \leq 1.5$ are similar to those of FCC phases, whereas the Ti-d electrons become more localized than those of δ phases in terms of a deeper pseudo-gap at Fermi level and sharper peaks below Fermi level. For the ε $TiH_{1.75}$ and TiH_2 phases, the DOS peaks become more localized and the states at the Fermi level are smaller than those of corresponding δ phases. All the above characteristics imply that the FCT TiH_x structure possess less metallic bonding and more covalent bonding than its FCC counterpart, which could, therefore, bring about a deep understanding to the bigger G/B value of the FCT structure shown in Fig. 5.

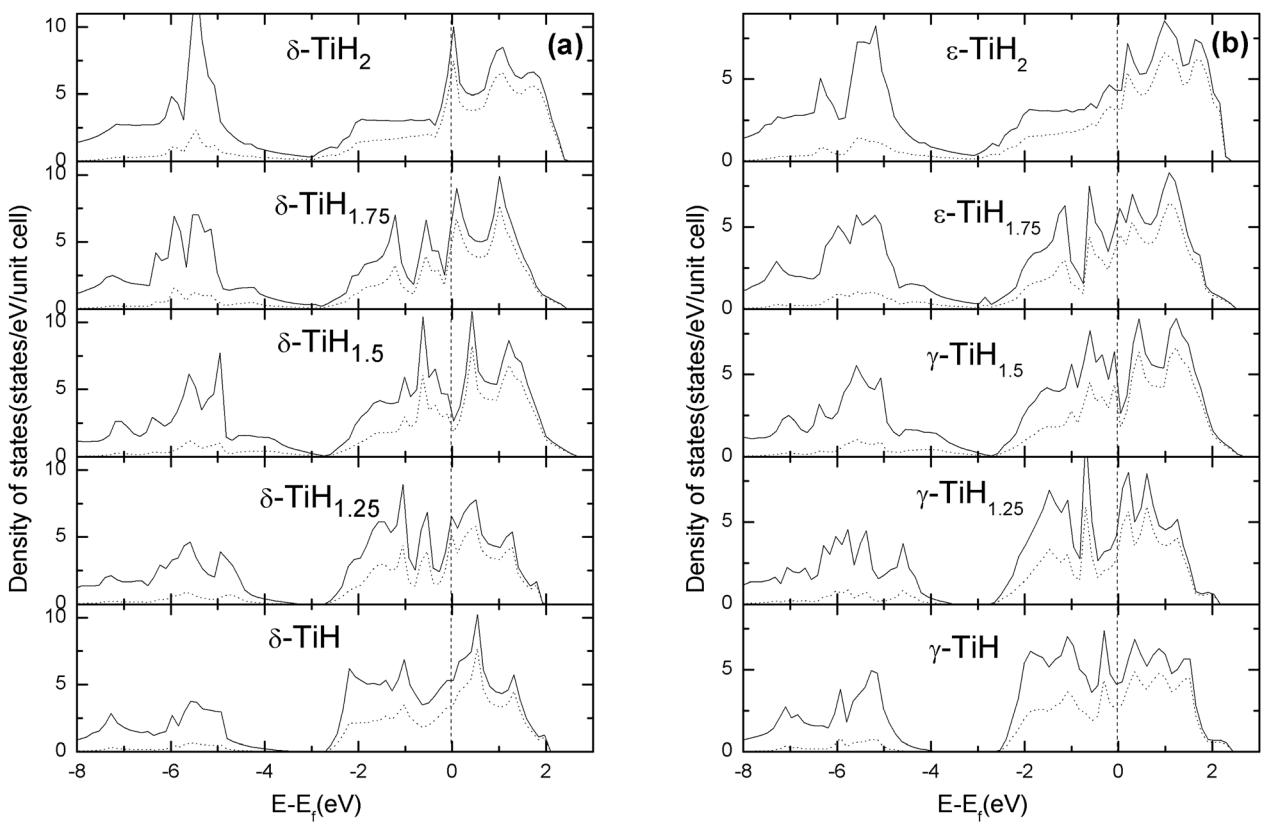

FIG. 6. Density of states of (a) FCC (δ) and (b) FCT (γ or ε) TiH_x phases with energetically favorable H atomic configurations. The solid and dashed lines are for total DOSs and Ti-d DOSs, respectively.

C. Thermodynamic property

The thermodynamic quantities are calculated by means of the quasi-harmonic Debye model and thermal electronic excitation. For a system at given volume (V) and temperature (T), the Helmholtz free energy $F(V,T)$ is obtained through combining electronic $F_{el}(V,T)$ and vibrational $F_{ph}(V,T)$ free energy[64,65]

$$F(V,T) = E_0(V) + F_{ph}(V,T) + F_{el}(V,T), \tag{6}$$

where $E_0(V)$ is the static total energy at 0 K. $F_{ph}(V,T)$ is given by the quasi-harmonic Debye model

$$F_{ph}(V,T) = n\left[\frac{9}{8}k_B\Theta_D(V) + 3k_BT\ln(1-e^{\Theta_D(V)/T}) - k_BTD(\Theta_D(V)/T)\right], \tag{7}$$

where $D(y)$ is the Debye integral defined as

$$D(y) = \frac{3}{y^3}\int_0^y \frac{x^3}{e^x-1}dx. \tag{8}$$

The Debye temperature Θ_D is expressed by

$$\Theta_D(V) = \frac{\hbar}{k_B}[6\pi^2V^{1/2}n]^{1/3}f(\nu)\sqrt{\frac{B}{M}}, \tag{9}$$

where n is the number of atoms per unit cell and M is the molecular mass per formula unit, B is the adiabatic bulk modulus, and $f(\nu)$ is given by

$$f(\nu) = \left\{3\left[2\left(\frac{2}{3}\frac{1+\nu}{1-2\nu}\right)^{3/2} + \left(\frac{1}{3}\frac{1+\nu}{1-\nu}\right)^{3/2}\right]^{-1}\right\}^{1/3}, \tag{10}$$

where v is the Poisson's ratio and calculated through Eq. (5). For TiH_2, the v is larger than 0.5 which is unphysical and is substituted by 0.33 for the Θ_D calculation. The electronic free energy $F_{el}(V,T)$ is written as

$$F_{el}(V,T) = E_{el}(V,T) - TS_{el}(V,T). \tag{11}$$

Thermal electronic energy, $E_{el}(V,T)$, can be calculated through

$$E_{el}(V,T) = \int g(\varepsilon,V)f(\varepsilon,V,T)\varepsilon d\varepsilon - \int g(\varepsilon,V)\varepsilon d\varepsilon, \tag{12}$$

where $f(\varepsilon,V,T)$ is the Fermi distribution and $g(\varepsilon,V)$ is electronic density of states. Electronic entropy, $S_{el}(V,T)$, is defined as

$$S_{el}(V,T) = -k_B\int g(\varepsilon,V)\{f(\varepsilon,V,T)\ln f(\varepsilon,V,T) + [1-f(\varepsilon,V,T)]\ln[1-f(\varepsilon,V,T)]\}\,d\varepsilon. \tag{13}$$

After the Helmholtz free energy is obtained at various volume, the volume as a function of temperature at ambient pressure, $V(T)_0$, is determined by fitting $F(V,T)$ into Vinet's equation of states (EOS)[66]

$$F(V,T) = F(V,T)_0 + \frac{4B(V,T)_0V(T)_0}{[B'(V,T)_0-1]^2} - \frac{2B(V,T)_0V(T)_0}{[B'(V,T)_0-1]^2} \times \left\{3[B'(V,T)_0-1]\left[\left(\frac{V(T)}{V(T)_0}\right)^{1/3}-1\right]+2\right\} \times \exp\left\{-\frac{3}{2}[B'(V,T)_0-1]\left[\left(\frac{V(T)}{V(T)_0}\right)^{1/3}-1\right]\right\}, \tag{14}$$

where $B(V,T)_0$ and $B'(V,T)$ are bulk modulus and pressure derivatives of bulk modulus, respectively. The coefficient of thermal expansion, $\alpha(T)$, is obtained by

$$\alpha(T) = \frac{1}{V(T)_0}\frac{\partial V(T)_0}{\partial T}. \tag{15}$$

The total isochoric heat capacity, C_V, is obtained by combining the contributions of electronic excitation C_{Vel} and phonon vibration C_{Vph} (Refs. 56 and 67)

$$C_V = C_{Vel} + C_{Vph}, \tag{16}$$

$$C_{Vel} = T\frac{\partial S_{el}(V,T)}{\partial T} = \gamma_eT, \tag{17}$$

and C_{Vph} can be divided into the contribution from Ti and H atoms,

$$C_{Vph} = C_{Vph}{}^{Ti} + C_{Vph}{}^{H}, \tag{18}$$

where $C_{Vph}{}^{Ti}$ and $C_{Vph}{}^{H}$ are calculated through the Debye and Einstein models,[56] respectively

$$C_{Vph}{}^{Ti} = 3n_{Ti}k_B\left[4D(\Theta_D/T) - \frac{3\Theta_D/T}{e^{\Theta_D/T}-1}\right], \tag{19}$$

$$C_{Vph}{}^{H} = 3n_HR(\Theta_E/T)^2e^{\Theta_E/T}/[e^{\Theta_E/T}-1]^2, \tag{20}$$

where $\Theta_E = h\upsilon_H/k_B$ is the Einstein temperature, R is the gas constant, n_{Ti} and n_H are the numbers of Ti and H atoms per formula unit, respectively. The isobaric heat capacity, C_P, is then calculated according to the following formula:[56,67]

$$C_P = C_V + \alpha^2BVT, \tag{21}$$

where B is the bulk modulus. After a series of calculations, the Θ_D, C_{Vel}, C_{Vph}, C_V, and C_P values are derived for FCC and FCT TiH_x phases at various temperatures. As typical examples, Table IV lists the heat capacities of FCC and FCT TiH_x phases with energetically favorable H atomic configurations at 300 K, Fig. 7 shows the heat capacities of δ TiH_2 as a function of temperature, and Fig. 8 summarizes the calculated coefficients of electronic heat capacities (γ_e) and Debye temperature (θ_D) of energetically favorable FCC and FCT TiH_x phases. In addition, the experimental values of δ TiH_x phases in the literature are also included in Table IV and Fig. 7 for the sake of comparison.[56,67–70] It should be pointed out that the C_P values of FCT structures are not

TABLE IV. Thermodynamic properties of FCC and FCT TiH_x phases with energetically favorable H configurations. θ_D is Debye temperature; γ_e, C_{Vph}, and C_P are coefficients of electronic isochoric heat capacity, phonon vibrational isochoric heat capacity, and isobaric heat capacity, respectively; α_L is coefficient of linear thermal expansion.

		θ_D (K)		Cv				α_L (10^{-6}/K)	
				γ_e (mJ/mol K)					
Phases	Structure	This study	Exp.	This study	Exp.	C_{Vph} (J/mol K)	C_P (J/mol K)	This study	Exp.
TiH_1	δ	492		3.36		25.43	27.41	15.60	
	γ	514		3.3		25.18			
$TiH_{1.25}$	δ	490	395 (Ref. 70)	2.92	3.11 (Ref. 70)	26.33	28.64	16.84	
	γ	495		2.85		26.28			
$TiH_{1.5}$	δ	523	385 (Ref. 70)	3.36	2.84 (Ref. 70)	26.83	28.83	17.66	
	γ	523	410 (Ref. 67)	3.38		26.83			
$TiH_{1.75}$	δ	311	293 (Ref. 70)	3.70	4.04 (Ref. 70)	29.85	32.52	18.89	
	ε	390	200 (Ref. 67)	2.98	3.53 (Ref. 69)	29.16			
TiH_2	δ	248	238 (Ref. 70)	5.07	5.10 (Ref. 70)	31.19	33.84	19.75	20 (Ref. 72)
	ε	408		3.08	4.53 (Ref. 69)	29.87			

given as their c/a ratio change with respect to volume changes.

Several features can be observed from Figs. 7 and 8 as well as from Table IV. First, the calculated thermodynamic quantities are consistent with the experimental results.[67–70] For instance, the present Θ_D value of δ TiH_2 is 248 K, which matches well with the corresponding value of 238.1 K from experiment.[70] One could also observe from Fig. 8(a) that for the FCC TiH_x phases, there is a sharp decrease of Θ_D when x is greater than 1.5, and such a decrease of Θ_D would bring about a softening of phonon spectrum and subsequent mechanical unstableness, which is consistent with the mechanically unstable FCC $TiH_{1.75}$ and TiH_2 phases revealed in Sec. III B.[70,71] Moreover, the FCT structure has a bigger Θ_D value than its FCC counterpart, especially for $TiH_{1.75}$ and TiH_2, and such a bigger Θ_D is originated from the increase of mechanical stability.[70–72]

Second, the C_{Vel} values of δ TiH_2 in Fig. 7 show an almost linear increase with the increase of temperature, and this characteristic could be understood through the coefficient of electronic heat capacity (γ_e). As shown in Fig. 8(b), the δ phases keep almost the same γ_e as the γ phases when $x \leq 1.5$, while have much bigger γ_e values as $x > 1.5$. It is known that γ_e is mainly determined by the density of states at Fermi level, i.e., $N(E_F)$[69,70]

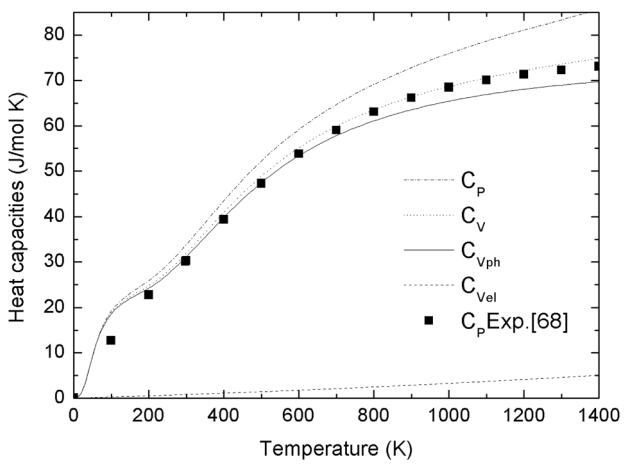

FIG. 7. Calculated total isochoric heat capacity (C_V), isobaric heat capacity (C_P), vibrational (C_{Vph}) and electronic (C_{Vel}) contributions of C_V for δ TiH_2 as a function of temperature. The solid cubes are experimental values.[68]

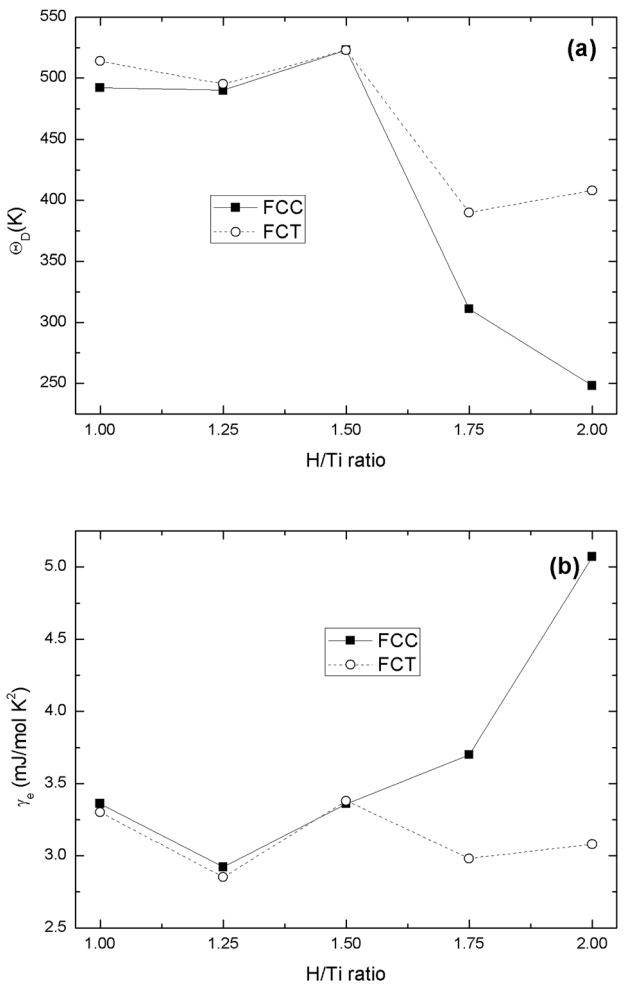

FIG. 8. Calculated coefficients of (a) Debye temperature (θ_D) and (b) electronic heat capacities (γ_e) of FCC and FCT TiH_x phases with energetically favorable H atomic configurations.

$$\gamma_e = (\pi/3)k^2 N(E_F)(1+\lambda). \quad (22)$$

From the above equation, it could be deduced that the bigger the $N(E_F)$, the higher the γ_e, which is consistent with the DOS and γ_e shown in Figs. 6 and 8, respectively. Moreover, the bigger $N(E_F)$ not only causes a higher γ_e but also results in instability of those phases at low temperature, which is called Jahn-Teller instability.

Third, the C_V values should play an important role in phase stability. It is well known that the free energy can be qualitatively estimated by heat capacities: the bigger the heat capacity, the lower the free energy with the increase of temperature. At low temperature, the heat capacity could be obtained through a simplified formula[70]

$$C_V \approx \frac{1}{\Theta_D{}^3} T^3 + \gamma_e T. \quad (23)$$

As mentioned before, the FCT TiH_x phase has bigger Θ_D and smaller γ_e than its FCC counterpart, and according to Eq. (23) the heat capacity of the FCT phase should be bigger. As a result, the free energy of the FCC phase would be lower than that of the FCT phase at high temperature, which will cause a phase transition from FCT to FCC. Furthermore, for each TiH_x phase, the differences of Θ_D and γ_e between δ and γ structures at $x \leq 1.5$ are much smaller than those between δ and ε phases at $x \geq 1.75$, and the differences of free energies would possibly follow the same trends as those of Θ_D and γ_e. Consequently, it would be expected that the $\gamma \rightarrow \delta$ transition will happen slower and at higher temperature than the $\varepsilon \rightarrow \delta$ transition, which agrees well with the experimental results in the literature.[2–4] In addition, the above statement could probably be the reason to the experimental observation why γ phase can exist in a temperature range of 0–441 K, while ε phase is only found below 310 K.[2–4]

Fourth, it can be seen from Fig. 7 that for the δ TiH_2 phase, the C_P values are bigger than corresponding C_V, and the difference between C_P and C_V increases with the increase of temperature. One could also observe from Fig. 7 that the calculated C_V values have a generally better agreement with experimental C_P values than the calculated C_P, and such a phenomenon is probably due to the fact that the experiment C_P values at high temperature were obtained through extrapolation of room-temperature data[68] to the traditional 3R rule. It should be mentioned that a good agreement between calculated C_V and experimental C_P was also found by Hu *et al.*[61]

Finally, the coefficient of volume thermal expansion (α) as a function of temperature is calculated according to Eq. (15), and the coefficient of linear thermal expansion (α_L) is obtained through the formula $\alpha_L = \alpha/3$. Accordingly, the obtained α_L values of δ TiH_x phases are listed in Table IV. It could be seen that the δ TiH_2 phase has a α_L value of 19.75×10^{-6}/K, which matches well with the experimental value of 20×10^{-6}/K.[73] Moreover, the α_L values of δ TiH_x phases are not only much bigger than that (8.6×10^{-6}/K) of pure Ti[1] but also increase with the increase of H concentration, suggesting that the addition of H could significantly increase thermal expansion of Ti. It should be noted that such a big α_L would make it very easy to the adsorption and dissociation of H atoms in the Ti lattice, while also causes a big volume change to Ti as hydrogen-storage materials.

IV. CONCLUDING REMARKS

First principle calculation has been conducted to investigate the atomic structure, mechanical properties, and thermodynamic quantities of various TiH_x phases. It is demonstrated that the TiH_x phases are energetically favorable with negative heats of formation, and H atoms occupy the atomic configuration of C_3 in $TiH_{1.5}$ due to the electronic and elastic properties. Calculation also shows that the H concentration has important effects on brittle/ductile behavior of TiH_x phases, and that the FCT structure is brittler than its FCC counterpart, indicating hydrogen embrittlement is easily found in FCT TiH_x phases with low H concentrations. In addition, the thermodynamic quantities show that the δ TiH_x phases experience much bigger thermal expansion than pure Ti, and the coefficient of thermal expansion of TiH_x increases as a function of H concentration. The calculated results agree well with experimental observations and could clarify the three controversies regarding TiH_x phases in the literature.

ACKNOWLEDGMENTS

This research work was supported by the Research Fund for the Doctoral Program of Higher Education of China (Grant No. 20110162110045), Key Project of Science and Technology of Hunan Province (Grant No. 2012FJ2003), and Scholarship Award for Excellent Doctoral Student granted by Ministry of Education of China and Hunan Provincial Innovation Foundation for Postgraduate (CX2011B112).

[1]G. Lütjering and J. C. Williams, *Titanium* (Springer, Heidelberg, 2007), Chap. 10.
[2]I. O. Bashkin, V. Y. Malyshev, and E. G. Ponyatovsky, Z. Phys. Chem. **179**, 111 (1993).
[3]F. D. Manchester and A. San-Martin, *in Phase Diagrams of Binary Hydrogen Alloys*, edited by F. D. Manchester (ASM International, USA, 2000), pp. 238–258.
[4]S. Ukita, H. Ohtani, and M. Hasebe, J. Jpn. Inst. Met. **71**, 721 (2007).
[5]R. Göring, R. Lukas, and K. Bohmhammel, J. Phys. C **14**, 5675 (1981).
[6]R. C. Frisch and R. A. Forman, J. Chem. Phys. **48**, 5187 (1968).
[7]E. Ehrenfreund, M. Weger, C. Korn, and D. Zamir, J. Chem. Phys. **50**, 1907 (1969).
[8]S. D. Goren, C. Korn, H. Riesemeier, E. Rössler, and K. Lüders, Phys. Rev. B **34**, 6917 (1986).
[9]C. Korn, Phys. Rev. B **17**, 1707 (1978).
[10]S. X. Tao, P. H. L. Notten, R. A. van Santen, and A. P. J. Jansen, Phys. Rev. B **79**, 144121 (2009).
[11]X. Q. Wang and J. T. Wang, Solid State Commun. **150**, 1715 (2010).
[12]Q. C. Xu and A. Van der Ven, Phys. Rev. B **76**, 064207 (2007).
[13]S. Martin and F. D. Manchester, Bull. Alloy Phase Diagrams **8**, 30 (1987).
[14]H. Okamoto, J. Phase Equilib. **32**, 174 (2011); **13**, 443 (1992).
[15]K. Wang, X. Kong, J. Dua, C. Li, Z. Li, and Z. Wu, CALPHAD: Comput. Coupling Phase Diagrams Thermochem. **34**, 317 (2010).
[16]H. Numakura and M. Koiwa, Acta Metall. **32**, 1799 (1984).
[17]H. Numakura, M. Koiwa, H. Asano, H. Murata, and F. Izumi, Scr. Metall. **20**, 213 (1986).
[18]C. P. Liang and H. R. Gong, "Fundamental mechanism of tetragonal transitions in titanium dihydride," Materials Chemistry and Physics (submitted).
[19]O. T. Woo and G. J. C. Carpenter, Scr. Metall. **19**, 931 (1985).
[20]R. Ding and I. P. Jones, J. Electron Microsc. **60**, 1 (2011).

[21]Y. Furuya, A. Takasaki, K. Mizuno, and T. Yoshiie, J. Alloys Compd. **446–447**, 447 (2007).
[22]C. Borchers, T. I. Khomenko, A. V. Leonov, and O. S. Morozova, Thermochim. Acta **493**, 80 (2009).
[23]E. Tal-Gutelmacher, R. Gemma, A. Pundt, and R. Kirchheim, Acta Mater. **58**, 3042 (2010).
[24]C. Q. Chen, S. X. Li, H. Zheng, L. B. Wang, and K. Lu, Acta Mater. **52**, 3697 (2004).
[25]M. I. Luppo, A. Politi, and G. Vigna, Acta Mater. **53**, 4987 (2005).
[26]V. N. Moiseyev, *Titanium Alloys: Russian Aircraft and Aerospace Applications* (Taylor & Francis, New York, 2006), Chap. 1.
[27]V. Madina and I. Azkarate, Int. J. Hydrogen Energy **34**, 5976 (2009).
[28]G. A. Lenning, C. M. Craighead, and R. I. Jaffee, Trans. AIME **200**, 367 (1954).
[29]E. Tal-Gutelmacher and D. Eliezer, JOM **57**, 46 (2005).
[30]C. L. Briant, Z. F. Wang, and N. Chollocoop, Corros. Sci. **44**, 1875 (2002).
[31]G. Kresse and J. Hafner, Phys. Rev. B **47**, 558 (1993).
[32]G. Kresse and J. Joubert, Phys. Rev. B **59**, 1758 (1999).
[33]J. P. Perdew, J. A. Chevary, S. H. Vosko, K. A. Jackson, M. R. Pederson, D. J. Singh, and C. Fiolhais, Phys. Rev. B **46**, 6671 (1992).
[34]M. Methfessel and A. T. Paxton, Phys. Rev. B **40**, 3616 (1989).
[35]P. E. Blöchl, O. Jepsen, and O. K. Andersen, Phys. Rev. B **49**, 16223 (1994).
[36]A. Togo, F. Oba, and I. Tanaka, Phys. Rev. B **78**, 134106 (2008).
[37]T. Wang, F. Eichhorn, D. Grambole, R. Grötzsche, F. Herrmann, U. Kreissig, and W. Möller, J. Phys.: Condens. Matter **14**, 11605 (2002).
[38]S. R. Peddada, I. M. Robertson, and H. K. Birnbaum, J. Mater. Res. **8**, 291 (1993).
[39]P. Millenbach and M. Givon, J. Less-Common. Met. **87**, 179 (1982).
[40]C. Korn, Phys. Rev. B **28**, 95 (1983).
[41]H. L. Yakel-Jr, Acta Cryst. **11**, 46 (1958).
[42]H. Zhang and E. H. Kisi, J. Phys.: Condens. Matter **9**, L185 (1997).
[43]Z. M. Azarkh and P. I. Gavrilov, Sov. Phys. Crystallogr. **15**, 231 (1970).
[44]R. L. Crane, S. C. Chattoraj, and M. B. Strope, J. Less-Common Met. **25**, 225 (1971).
[45]P. E. Irving and C. J. Beevers, Metall. Trans. **2**, 613 (1971).
[46]J. H. Weaver, D. J. Peterman, D. T. Peterson, and A. Franciosi, Phys. Rev. B **23**, 1692 (1981).
[47]M. Arita, K. Shimizu, and Y. Ichinose, Metall. Trans. A **13**, 1329 (1982).
[48]M. Arita and M. Someno, J. Chem. Eng. Data **24**, 277 (1979).
[49]T. Nishikiori, T. Nohira, and Y. Ito, J. Electrochem. Soc. **148**, E38 (2001).
[50]R. M. Haag and F. J. Shipko, J. Am. Chem. Soc. **78**, 5155 (1956).
[51]W. E. Wang, J. Alloys Compd. **238**, 6 (1996).
[52]J. K. Kivilahti and J. M. Miettinen, CALPHAD: Comput. Coupling Phase Diagrams Thermochem. **11**, 187 (1987).
[53]E. Königsberger, G. Eriksson, and W. A. Oates, J. Alloys Compd. **299**, 148 (2000).
[54]C. A. Chen, Y. Sun, H. Y. Wang, W. D. Xue, and Z. H. Zhu, Chin. J. At. Mol. Phys. **18**, 377 (2001).
[55]J. W. Zhao, H. Ding, X. F. Tian, W. J. Zhao, and H. L. Hou, Chin. J. Chem. Phys. **21**, 569 (2008).
[56]D. Setoyama, J. Matsunaga, H. Muta, M. Uno, and S. Yamanaka, J. Alloys Compd. **381**, 215 (2004).
[57]M. H. Sadd, *Elasticity: Theory, Applications, Numerics* (Elsevier Inc., USA, 2005), pp. 291–292.
[58]R. Yu, J. Zhu, and H. Q. Ye, Comput. Phys. Commun. **181**, 671 (2010).
[59]P. E. Kalita, S. V. Sinogeikin, K. Lipinska-Kalita, T. Hartmann, X. Ke, C. Chen, and A. Cornelius, J. Appl. Phys. **108**, 043511 (2010).
[60]P. E. Kalita, A. L. Cornelius, K. E. Lipinska-Kalita, C. L. Gobin, and H. P. Liermann, J. Phys. Chem. Solids **69**, 2240 (2008).
[61]C. H. Hu, D. M. Chen, Y. M. Wang, and K. Yang, J. Alloys Compd. **450**, 369 (2008).
[62]S. F. Pugh, Philos. Mag. **45**, 823 (1954).
[63]K. S. Chan, Acta Metall. **43**, 4325 (1995).
[64]Y. Wang, J. J. Wang, H. Zhang, V. R. Manga, S. L. Shang, L. Q. Chen, and Z. K. Liu, J. Phys.: Condens. Matter **22**, 225404 (2010).
[65]A. Otero-de-la-Roza, D. Abbasi-Pérez, and V. Luaña, Comput. Phys. Commun. **182**, 2232 (2011).
[66]P. Vinet, J. Ferrante, J. R. Smith, and J. H. Rose, J. Phys. C **19**, L467 (1986).
[67]D. Setoyama, J. Matsunaga, M. Ito, H. Muta, K. Kurosaki, M. Uno, and S. Yamanaka, J. Nucl. Mater. **344**, 298 (2005).
[68]M. W. Chase-Jr, *NIST. JANAF Thermochemical Tables*, 4th ed. (National Institute of Standards and Technology, Maryland, 1998).
[69]J. Li, A. Pflaum, F. Pobell, and P. Sekowski, J. Low Temp. Phys. **88**, 309 (1992).
[70]K. Bohmhammel, G. Wolf, G. Gross, and H. Midge, J. Low Temp. Phys. **43**, 521 (1981).
[71]M. T. Dove, *Introduction to Lattice Dynamics* (Cambridge University Press, Cambridge, UK, 1993).
[72]J. Bhattacharya and A. Van der Ven, Acta Mater. **56**, 4226 (2008).
[73]G. F. Kobzenko, A. P. Kobzenko, M. V. Chubenko, V. V. PetKov, and A. V. Polenur, Int. J. Hydrogen Energy **20**, 383 (1995).